

# The simplest normal form and its application to bifurcation control

Pei Yu <sup>a,\*</sup>, A.Y.T. Leung <sup>b</sup>

<sup>a</sup> *Department of Applied Mathematics, The University of Western Ontario, London, ON, Canada N6A 5B7*

<sup>b</sup> *Department of Building and Construction, The City University of Hong Kong, Kowloon, Hong Kong*

Accepted 29 December 2005

---

## Abstract

This paper is concerned with the computation of the simplest normal forms with perturbation parameters, associated with codimension-one singularities, and applications to control systems. First, an efficient method is presented to compute the normal forms for general semi-simple cases, which combines center manifold theory and normal form theory in one unified procedure. The efficient approach is then applied to find the explicit simplest normal forms of general  $n$ -dimensional nonlinear dynamical systems whose Jacobian matrices evaluated at an equilibrium point contain either single zero or a purely imaginary pair. In addition to near-identity nonlinear transformation, time and parameter rescalings are used to obtain the simplest normal forms. It is shown that, unlike the classical normal forms, the simplest normal forms for single zero and Hopf singularities are finite up to an arbitrary order, which greatly simplify stability and bifurcation analysis. The new method is applied to consider controlling bifurcations of the Lorenz system and a nonlinear electrical circuit. Symbolic programs have been developed using Maple, which greatly facilitates applications.

© 2006 Elsevier Ltd. All rights reserved.

---

## 1. Introduction

Normal form theory is one of the useful tools in the study of nonlinear dynamical systems and often applied to control systems to consider instability and bifurcation control (for example, see [1–8]). A control system can be described by a map, a function or, in more general, an operator in either time domain or frequency domain. Differential equations are the most useful and widely applied tools in describing control systems. They may be ordinary differential equations, partial differential equations, delayed differential equations, or combination of differential equations and algebraic equations. In this paper, the attention is focused on control systems described by ordinary differential equations.

The main idea of normal form theory is to apply successive coordinate transformations to systematically construct a form of the original system as simple as possible. The new form is qualitatively equivalent to the original system and thus the dynamical analysis of the original system is greatly simplified. However, a conventional normal form (CNF) is in general not unique and can be further simplified using similar near-identity transformations, leading to the simplest normal form (SNF). For example, the CNF of Hopf bifurcation contains an infinite number of terms while the SNF of

---

\* Corresponding author. Tel.: +1 519 661 2111; fax: +1 519 661 3523.  
E-mail address: [pyu@pyu1.apmaths.uwo.ca](mailto:pyu@pyu1.apmaths.uwo.ca) (P. Yu).

Hopf singularity without unfolding has only three terms up to an arbitrary order. Such further reductions have recently received considerable attention [9–21]. Roughly speaking, the main difference between the CNF and the SNF can be explained from the computation point of view: for the CNF, the coefficients of the  $k$ th order nonlinear transformation are only used to possibly remove the  $k$ th order nonlinear terms of the system; while for the SNF, the  $k$ th order nonlinear transformation coefficients are not only used to simplify the  $k$ th order terms of the system, but also used to eliminate higher order nonlinear terms. In general, the SNF computation is much more complicated than that of the CNF, and computer algebra systems such as Maple, Mathematica, Reduce, etc. must be used [14,15,18–20]. However, even with the aid of computer algebra systems, computational efficiency is still the main concern in computing the SNF. Therefore, attention has been paid to developing efficient methodologies and efficient algorithms for the computation of the SNF [22–25].

The computation of normal forms has been mainly restricted to systems which do not contain perturbation parameters (unfolding). However, in practice a physical system or a control problem always involves some parameters, usually called perturbation parameters or unfolding. Such normal forms are very important in applications. A CNF with unfolding is usually obtained in two steps: First ignore the perturbation parameter and compute the normal form for the corresponding “reduced” system (by setting the parameters zero), and then add an unfolding to the resulting normal form. This way it greatly reduces the computation effort, with the cost that it does not provide the transformation between the original system and the normal form. For the SNF, on the other hand, since Ushiki [9] introduced the method of infinitesimal deformation in 1984 to study the SNF of vector fields, although many researchers have considered several cases of singularities (for example, see [9–14,16,17,20]), no single application using the SNF has been reported. This is because that the main attention in this area has been focused on the computation of the SNF without perturbation parameters. Recently, single zero and Hopf singularities have been considered and the explicit SNFs with unfolding have been obtained by introducing time and parameter rescalings [22,26]. However, the systems considered in these two papers are assumed on center manifolds. This is not convenient in applications since practical systems are usually not described on center manifold. This restriction will be removed in this paper, and the SNFs associated with dimension-one singularities (either single zero or Hopf) will be derived from general  $n$ -dimensional nonlinear differential equations.

For a general nonlinear physical or engineering system, which may include stable manifold, normal form theory is usually employed together with center manifold theory [27] in order to take the contribution from the stable manifold. In general, given a nonlinear system, center manifold theory is applied before employing normal form theory. The idea of center manifold theory is similar to normal form theory—simplify the system by applying successive nonlinear transformations. It reduces the original system to a center manifold which has smaller dimension than that of the original system. Different methods have been developed to combine center manifold theory with normal form theory in one unified procedure (e.g., see [23,26,28]). In [23] an efficient computation method and Maple programs are developed for general systems associated with semi-simple cases. However, the normal form computation presented in [23] does not contain perturbation parameters (unfolding), and thus is not directly applicable in solving practical problems.

In this paper, we will develop an efficient approach for computing the SNF with perturbation parameters (unfolding) directly from general  $n$ -dimensional systems which are not necessarily described on center manifold, and apply the method to consider controlling bifurcations. An explicit, recursive formula will be derived for computing the normal forms associated with general semi-simple cases. The approach is efficient since it reduces the computation to minimum at each step of finding ordered algebraic equations. Based on the general recursive formula, the SNFs for single zero and Hopf singularities are obtained. The rest of the paper is organized as follows. In the next section, the general formulas for computing the center manifolds, normal forms and nonlinear transformations of general semi-simple cases are derived. The SNFs for the single zero and Hopf singularity are obtained in Section 3. The applications to bifurcation control are presented in Section 4 to show the efficiency of the method. Finally, conclusions are drawn in Section 5.

## 2. General formulation

In this section, we shall derive the explicit formulas for computing the normal forms associated with semi-simple cases. Consider the following general control system, given by

$$\frac{dx}{dt} = F(x, \mu) + u, \quad x, u \in R^n, \mu \in R^s, F: R^n \rightarrow R^n, \quad (1)$$

where  $x$ ,  $u$  and  $\mu$  are state variable, control variable and system parameter, respectively.  $\mu$  may be considered as control parameters. Usually,  $\mu$  is not explicitly shown in a control system. In this paper,  $\mu$  is explicitly shown for the convenience of bifurcation analysis. The control function  $u$  can be, in general, any kind of function of the parameter  $\mu$  as

well as time  $t$ , which renders system (1) non-autonomous. However, when a control law is determined, system (1) may be transformed to autonomous. For instance, suppose the feedback, given by

$$\mathbf{u} = \mathbf{u}(\mathbf{x}, \boldsymbol{\mu}), \tag{2}$$

is chosen, then system (1) becomes autonomous, and the bifurcation theory for differential equations can be applied with the  $\boldsymbol{\mu}$  as control parameter. Then, Eq. (1) can be rewritten as

$$\frac{d\mathbf{x}}{dt} = \mathbf{F}(\mathbf{x}, \boldsymbol{\mu}) + \mathbf{u}(\mathbf{x}, \boldsymbol{\mu}) \triangleq \mathbf{J}\mathbf{x} + \mathbf{f}(\mathbf{x}, \boldsymbol{\mu}), \quad \mathbf{x} \in \mathbf{R}^n, \boldsymbol{\mu} \in \mathbf{R}^s, \tag{3}$$

where  $\mathbf{J}\mathbf{x}$  denotes the linear terms. Further, without loss of generality, it is assumed that  $\mathbf{x} = \mathbf{0}$  is an equilibrium point of the system for any values of  $\boldsymbol{\mu}$ , i.e.,  $\mathbf{f}(\mathbf{0}, \boldsymbol{\mu}) \equiv \mathbf{0}$ . The nonlinear function  $\mathbf{f}$  is assumed analytic with respect to  $\mathbf{x}$  and  $\boldsymbol{\mu}$ .  $\mathbf{J}$  is the Jacobian matrix of the system evaluated at the equilibrium point  $\mathbf{x} = \mathbf{0}$ , when the parameter  $\boldsymbol{\mu}$  reaches its critical point  $\boldsymbol{\mu} = \mathbf{0}$ , given in the form of

$$\mathbf{J} = \begin{bmatrix} J_0 & 0 \\ 0 & J_1 \end{bmatrix}, \tag{4}$$

where both  $J_0$  and  $J_1$  are assumed in diagonal form, indicating that all the eigenvalues of the Jacobian are semi-simple.  $J_0$  includes the eigenvalues  $\lambda_1, \lambda_2, \dots, \lambda_{n_0}$  with zero real parts, while  $J_1$  has the eigenvalues  $\lambda_{n_0+1}, \lambda_{n_0+2}, \dots, \lambda_n$  with negative real parts. In other words, system (3) does not contain unstable manifold in the vicinity of  $\mathbf{x}$ .

To find the normal form of system (3), one may expand the dimension of system (3) from  $n$  to  $n + s$ , by adding the equation  $\frac{d\boldsymbol{\mu}}{dt} = \mathbf{0}$  to system (3) to obtain a new system:

$$\frac{d\mathbf{x}}{dt} = \mathbf{J}\mathbf{x} + \mathbf{f}(\mathbf{x}, \boldsymbol{\mu}), \quad \frac{d\boldsymbol{\mu}}{dt} = \mathbf{0}, \quad \mathbf{x} \in \mathbf{R}^n, \boldsymbol{\mu} \in \mathbf{R}^s. \tag{5}$$

Then a general near-identity transformation may be assumed either in the form of

$$\mathbf{x} = \mathbf{y} + \mathbf{h}(\mathbf{y}, \mathbf{v}), \quad \boldsymbol{\mu} = \mathbf{v}, \tag{6}$$

or

$$\mathbf{x} = \mathbf{y} + \mathbf{h}_1(\mathbf{y}, \mathbf{v}), \quad \boldsymbol{\mu} = \mathbf{v} + \mathbf{h}_2(\mathbf{y}, \mathbf{v}), \tag{7}$$

where  $\mathbf{h}(\mathbf{y}, \mathbf{v})$ ,  $\mathbf{h}_1(\mathbf{y}, \mathbf{v})$  and  $\mathbf{h}_2(\mathbf{y}, \mathbf{v})$  are nonlinear analytic functions of  $\mathbf{y}$  and  $\mathbf{v}$ . The equation  $\boldsymbol{\mu} = \mathbf{v}$  given in Eq. (6) emphasizes that the parameter  $\boldsymbol{\mu}$  is not changed under the transformation (6), i.e., reparametrization is not applied. For convenience, we may call transformation (6) as *state transformation* since it only changes state variable  $\mathbf{x}$ , while call Eq. (7) as *state-parameter transformation* because the parameter  $\boldsymbol{\mu}$  is also expressed in terms of both  $\mathbf{y}$  and  $\mathbf{v}$ . The state transformation is a natural way from the physical point of view since the parameter  $\mathbf{v}$  is not a function of time. The state-parameter transformation however contains time variation in parameter  $\boldsymbol{\mu}$  since it involves the state variable  $\mathbf{y}$ . In this paper we only consider the near-identity state transformation or simply near-identity (nonlinear) transformation (6) but with reparametrization  $\boldsymbol{\mu} = \mathbf{v} + \mathbf{p}(\mathbf{v})$ . Thus, transformation (6) becomes

$$\mathbf{x} = \mathbf{y} + \mathbf{h}(\mathbf{y}, \mathbf{v}), \quad \boldsymbol{\mu} = \mathbf{v} + \mathbf{p}(\mathbf{v}). \tag{8}$$

For the transformation (8), we can show that it is not necessary to extend the  $n$ -dimensional system (3) to  $(n + s)$ -dimensional system (5). In fact directly apply normal form theory to system (3) is equivalent to using system (5). To prove this, we assume that the transformed system (normal form) is given by

$$\frac{d\mathbf{y}}{dt} = \mathbf{J}\mathbf{y} + \mathbf{g}(\mathbf{y}, \mathbf{v}), \quad \frac{d\mathbf{v}}{dt} = \mathbf{0}. \tag{9}$$

Then differentiating the first equation of (9) with respect to  $t$  results in  $\frac{d\mathbf{x}}{dt} = \frac{d\mathbf{y}}{dt} + \frac{\partial \mathbf{h}}{\partial \mathbf{y}} \frac{d\mathbf{y}}{dt} + \frac{\partial \mathbf{h}}{\partial \mathbf{v}} \frac{d\mathbf{v}}{dt}$  and then substituting Eqs. (5) and (9) into the resulting equation yields

$$\left( 1 + \frac{\partial \mathbf{h}}{\partial \mathbf{y}} \right) \mathbf{g}(\mathbf{y}, \mathbf{v}) = \mathbf{L}\mathbf{h}(\mathbf{y}, \mathbf{v}) - \frac{\partial \mathbf{h}}{\partial \mathbf{y}} \mathbf{J}\mathbf{y} + \mathbf{f}(\mathbf{y} + \mathbf{h}(\mathbf{y}, \mathbf{v}), \mathbf{v}). \tag{10}$$

Then the computation of the normal form of system (5) completely depends upon Eq. (10). However, it is easy to see that Eq. (10) can be also directly derived from Eq. (3) with the aid of the first equations of (6) and (9). Therefore, in this paper we shall use Eq. (3).

Now back to the original system (3), and let  $\mathbf{x} = (\mathbf{x}_1, \mathbf{x}_2)^T$ , where  $\mathbf{x}_1$  and  $\mathbf{x}_2$  are variables associated with the eigenvalues of  $J_0$  and  $J_1$ , respectively. Then, Eq. (3) can be rewritten as

$$\begin{aligned}\frac{dx_1}{dt} &= J_0 x_1 + f_1(x_1, x_2, \mu), \\ \frac{dx_2}{dt} &= J_1 x_2 + f_2(x_1, x_2, \mu).\end{aligned}\quad (11)$$

By center manifold theory [27],  $x_2$  can be expressed in terms of  $x_1$  as

$$x_2 = N(x_1, \mu), \quad \text{satisfying } N(\mathbf{0}, \mathbf{0}) = \mathbf{0}, \quad \frac{\partial N(\mathbf{0}, \mathbf{0})}{\partial x_1 \partial \mu} = 0, \quad (12)$$

under which the second equation of (11) can be rewritten as

$$D_{x_1} N(x_1, \mu) [J_0 x_1 + f_1(x_1, N(x_1, \mu), \mu)] = J_1 N(x_1, \mu) + f_2(x_1, N(x_1, \mu), \mu). \quad (13)$$

Having found  $N(x_1, \mu)$  from the above equation, the first equation of (11) becomes

$$\frac{dx_1}{dt} = J_0 x_1 + f_1(x_1, N(x_1, \mu), \mu), \quad (14)$$

which governs the dynamics of the original system (3) in the vicinity of  $(x, \mu) = (\mathbf{0}, \mathbf{0})$ .

In order to further simplify Eq. (14), introduce the following nonlinear transformation

$$x_1 = w + H(w, v) \triangleq w + \sum_{m=2}^{\infty} H_m(w, v), \quad (15)$$

and the time rescaling

$$t = (T_0 + T(w, v))\tau \triangleq \tau + \sum_{m=1}^{\infty} T_m(w, v)\tau, \quad (16)$$

where  $v$  indicates the parameter rescaling, given in the form of

$$\mu = v + p(v) \triangleq v + \sum_{m=2}^{\infty} p_m(v). \quad (17)$$

Note that unlike the transformation (7), here  $\mu$  given in Eq. (17) does not involve the time variable  $w$ . Also note that  $T_0$  has been taken as 1 for convenience.

Further, assume that the normal form of system (14) is given by

$$\frac{dw}{d\tau} = J_0 w + C(w, v) \triangleq J_0 w + \sum_{m=2}^{\infty} C_m(w, v). \quad (18)$$

Here,  $H_m(w, v)$  and  $C_m(w, v)$  are the  $m$ th degree,  $n_0$ -dimensional vector homogeneous polynomials of  $w$  and  $v$ , and  $p_m(v)$  is the  $m$ th degree,  $s$ -dimensional vector homogeneous polynomials of  $v$ , while  $T_m(w, v)$  is the  $m$ th degree, scalar homogeneous polynomials of its components.

To find the normal form, first differentiating Eq. (15) and substituting it into Eq. (14) yields

$$(I + D_w H(w, v)) \frac{dw}{d\tau} = \frac{dt}{d\tau} [J_0(w + H(w, v)) + f_1(w + H(w, v), N(w + H(w, v), v + p(v)), v + p(v))], \quad (19)$$

and then using Eq. (16) and substituting Eq. (10) into the above equation and rearranging results in

$$\begin{aligned}D_w H(w, v) J_0 w - J_0 H(w, v) &= f_1(w + H(w, v), h(w, v), v + p(v)) - D_w H(w, v) C(w, v) - C(w, v) \\ &\quad + T(w, v) [J_0(w + H(w, v)) + f_1(w + H(w, v), h(w, v), v + p(v))],\end{aligned}\quad (20)$$

where  $h(w, v) \equiv N(w + H(w, v), v + p(v))$ .

Next, one may substitute Eq. (15) into Eq. (13), and use Eq. (20) to find the following equation:

$$\begin{aligned}D_{x_1} N(x_1, \mu) \{ (I + D_w H(w, v)) (J_0 w + C(w, v)) - T(w, v) [J_0(w + H(w, v)) \\ + f_1(w + H(w, v), h(w, v), v + p(v))] \} &= J_1 h(w, v) + f_2(w + H(w, v), h(w, v), v + p(v)).\end{aligned}\quad (21)$$

By chain rule,  $D_{x_1} N(x_1, v) (I + D_w H(w, v)) = D_w h(w, v)$ , one can rewrite Eq. (21) as

$$\begin{aligned}D_w h(w, v) J_0 w - J_1 h(w, v) &= f_2(w + H(w, v), h(w, v), v + p(v)) - D_w h(w, v) C(w, v) \\ &\quad + T(w, v) D_w h(w, v) [I + D_w H(w, v)]^{-1} [J_0(w + H(w, v)) \\ &\quad + f_1(w + H(w, v), h(w, v), v + p(v))].\end{aligned}\quad (22)$$

Finally, combining Eqs. (20) and (22) yields the following compact form:

$$\begin{aligned}
 D \begin{pmatrix} \mathbf{H}(\mathbf{w}, \mathbf{v}) \\ \mathbf{h}(\mathbf{w}, \mathbf{v}) \end{pmatrix} J_0 \mathbf{w} - \begin{bmatrix} J_0 & 0 \\ 0 & J_1 \end{bmatrix} \begin{pmatrix} \mathbf{H}(\mathbf{w}, \mathbf{v}) \\ \mathbf{h}(\mathbf{w}, \mathbf{v}) \end{pmatrix} &= \begin{pmatrix} \mathbf{f}_1(\mathbf{w} + \mathbf{H}(\mathbf{w}, \mathbf{v}), \mathbf{h}(\mathbf{w}, \mathbf{v}), \mathbf{v} + \mathbf{p}(\mathbf{v})) \\ \mathbf{f}_2(\mathbf{w} + \mathbf{H}(\mathbf{w}, \mathbf{v}), \mathbf{h}(\mathbf{w}, \mathbf{v}), \mathbf{v} + \mathbf{p}(\mathbf{v})) \end{pmatrix} - D \begin{pmatrix} \mathbf{H}(\mathbf{w}, \mathbf{v}) \\ \mathbf{h}(\mathbf{w}, \mathbf{v}) \end{pmatrix} \mathbf{C}(\mathbf{w}, \mathbf{v}) \\
 &\quad - \begin{pmatrix} \mathbf{C}(\mathbf{w}, \mathbf{v}) \\ \mathbf{0} \end{pmatrix} + T(\mathbf{w}, \mathbf{v}) \begin{bmatrix} I \\ D\mathbf{h}(\mathbf{w}, \mathbf{v})[I + D\mathbf{H}(\mathbf{w}, \mathbf{v})]^{-1} \end{bmatrix} [J_0(\mathbf{w} + \mathbf{H}(\mathbf{w}, \mathbf{v})) \\
 &\quad + \mathbf{f}_1(\mathbf{w} + \mathbf{H}(\mathbf{w}, \mathbf{v}), \mathbf{h}(\mathbf{w}, \mathbf{v}), \mathbf{v} + \mathbf{p}(\mathbf{v}))], \tag{23}
 \end{aligned}$$

where the differential operator  $D \equiv D_{\mathbf{w}}$ .

Eq. (23) is all what we need for computing the normal form  $\mathbf{C}(\mathbf{w}, \mathbf{v})$ , the nonlinear transformations  $\mathbf{H}(\mathbf{w}, \mathbf{v})$  and  $\mathbf{h}(\mathbf{w}, \mathbf{v})$  as well as the time rescaling  $T(\mathbf{w}, \mathbf{v})$  and the reparametrization  $\mathbf{p}(\mathbf{v})$ . Note that all  $\mathbf{C}(\mathbf{w}, \mathbf{v})$ ,  $\mathbf{H}(\mathbf{w}, \mathbf{v})$  and  $\mathbf{h}(\mathbf{w}, \mathbf{v})$  start from second order terms and can be expressed in terms of vector homogeneous polynomials of  $\mathbf{w}$  and  $\mathbf{v}$ .  $\mathbf{C}(\mathbf{w}, \mathbf{v})$  and  $\mathbf{H}(\mathbf{w}, \mathbf{v})$  are  $n_0$ -dimensional vectors while  $\mathbf{h}(\mathbf{w}, \mathbf{v})$  is a  $(n - n_0)$ -dimensional vector.  $T(\mathbf{w}, \mathbf{v})$  is a scalar function while  $\mathbf{p}(\mathbf{v})$  is a  $s$ -dimensional vector.

Since, in general, it is not possible to find the closed-form solutions for  $\mathbf{C}(\mathbf{w}, \mathbf{v})$ ,  $\mathbf{H}(\mathbf{w}, \mathbf{v})$ ,  $\mathbf{h}(\mathbf{w}, \mathbf{v})$ ,  $T(\mathbf{w}, \mathbf{v})$  and  $\mathbf{p}(\mathbf{v})$  from Eq. (22), we may assume the approximate solutions, given by

$$\begin{aligned}
 \mathbf{C}(\mathbf{w}, \mathbf{v}) &= \sum_{m=2}^{\infty} \mathbf{C}_m(\mathbf{w}, \mathbf{v}) = \sum_{m=2}^{\infty} \sum_m \mathbf{C}_m w_1^{m_1} \cdots w_{n_0}^{m_{n_0}} v_1^{m_{n_0+1}} \cdots v_s^{m_{n_0+s}}, \\
 \mathbf{H}(\mathbf{w}, \mathbf{v}) &= \sum_{m=2}^{\infty} \mathbf{H}_m(\mathbf{w}, \mathbf{v}) = \sum_{m=2}^{\infty} \sum_m \mathbf{H}_m w_1^{m_1} \cdots w_{n_0}^{m_{n_0}} v_1^{m_{n_0+1}} \cdots v_s^{m_{n_0+s}}, \tag{24} \\
 \mathbf{h}(\mathbf{w}, \mathbf{v}) &= \sum_{m=2}^{\infty} \mathbf{h}_m(\mathbf{w}, \mathbf{v}) = \sum_{m=2}^{\infty} \sum_m \mathbf{h}_m w_1^{m_1} \cdots w_{n_0}^{m_{n_0}} v_1^{m_{n_0+1}} \cdots v_s^{m_{n_0+s}},
 \end{aligned}$$

and

$$\begin{aligned}
 T(\mathbf{w}, \mathbf{v}) &= \sum_{m=1}^{\infty} T_m(\mathbf{w}, \mathbf{v}) = \sum_{m=1}^{\infty} \sum_m T_m w_1^{m_1} \cdots w_{n_0}^{m_{n_0}} v_1^{m_{n_0+1}} \cdots v_s^{m_{n_0+s}}, \tag{25} \\
 \mathbf{p}(\mathbf{v}) &= \sum_{m=2}^{\infty} \mathbf{p}_m(\mathbf{v}) = \sum_{m=2}^{\infty} \sum_m \mathbf{p}_m v_1^{m_1} v_2^{m_2} \cdots v_s^{m_s},
 \end{aligned}$$

where  $\mathbf{C}_m$ ,  $\mathbf{H}_m$ ,  $\mathbf{h}_m$ ,  $T_m$  and  $\mathbf{p}_m$  represent the  $m$ th order coefficients. The subscript  $m$  means that for all possible non-negative integers,  $m_1, m_2, \dots, m_{n_0+s}$  satisfy  $m_1 + m_2 + \dots + m_{n_0+s} = m$  (or  $m_1 + m_2 + \dots + m_s = m$  for  $\mathbf{p}_m$ ).

Further, for an arbitrary  $m \geq 2$ , one can show that

$$\begin{aligned}
 D \begin{pmatrix} \mathbf{H}_m(\mathbf{w}, \mathbf{v}) \\ \mathbf{h}_m(\mathbf{w}, \mathbf{v}) \end{pmatrix} J_0 \mathbf{w} &= \sum_m D \begin{pmatrix} \mathbf{H}_m \\ \mathbf{h}_m \end{pmatrix} w_1^{m_1} \cdots w_{n_0}^{m_{n_0}} v_1^{m_{n_0+1}} \cdots v_s^{m_{n_0+s}} (J_0 \mathbf{w}) \\
 &= \sum_m \left[ \sum_{i=1}^{n_0} \frac{\partial}{\partial w_i} \begin{pmatrix} \mathbf{H}_m \\ \mathbf{h}_m \end{pmatrix} w_1^{m_1} \cdots w_{n_0}^{m_{n_0}} v_1^{m_{n_0+1}} \cdots v_s^{m_{n_0+s}} \lambda_i w_i \right] \\
 &= \sum_m (m_1 \lambda_1 + \cdots + m_{n_0} \lambda_{n_0}) \begin{pmatrix} \mathbf{H}_m \\ \mathbf{h}_m \end{pmatrix} w_1^{m_1} \cdots w_{n_0}^{m_{n_0}} v_1^{m_{n_0+1}} \cdots v_s^{m_{n_0+s}} \\
 &= \sum_m \lambda_0 \begin{pmatrix} \mathbf{H}_m \\ \mathbf{h}_m \end{pmatrix} w_1^{m_1} \cdots w_{n_0}^{m_{n_0}} v_1^{m_{n_0+1}} \cdots v_s^{m_{n_0+s}} = \lambda_0 \begin{pmatrix} \mathbf{H}_m(\mathbf{w}, \mathbf{v}) \\ \mathbf{h}_m(\mathbf{w}, \mathbf{v}) \end{pmatrix}, \tag{26}
 \end{aligned}$$

where

$$\lambda_0 = m_1 \lambda_1 + m_2 \lambda_2 + \cdots + m_{n_0}. \tag{27}$$

Thus, one can obtain the following equation from Eq. (23) for solving the  $m$ th order coefficients:  $\mathbf{C}_m$ ,  $\mathbf{H}_m$ ,  $\mathbf{h}_m$ ,  $T_m$  and  $\mathbf{p}_m$ :

$$\begin{pmatrix} [\lambda_0 I - J_0] \mathbf{H}_m \\ [\lambda_0 I - J_1] \mathbf{h}_m \end{pmatrix} = \begin{pmatrix} \tilde{\mathbf{f}}_{1m} \\ \tilde{\mathbf{f}}_{2m} \end{pmatrix} - \begin{pmatrix} \mathbf{C}_m \\ \mathbf{0} \end{pmatrix}, \tag{28}$$

where the  $m$ th order coefficients  $\tilde{f}_{1m}$  and  $\tilde{f}_{2m}$  are extracted from

$$\tilde{f}_1 = f_1(\mathbf{w} + \mathbf{H}(\mathbf{w}, \mathbf{v}), \mathbf{h}(\mathbf{w}, \mathbf{v}), \mathbf{v} + \mathbf{p}(\mathbf{w})) - D\mathbf{H}(\mathbf{w}, \mathbf{v})\mathbf{C}(\mathbf{w}, \mathbf{v}) + T(\mathbf{w}, \mathbf{v})[J_0(\mathbf{w} + \mathbf{H}(\mathbf{w}, \mathbf{v})) + f_1(\mathbf{w} + \mathbf{H}(\mathbf{w}, \mathbf{v}), \mathbf{h}(\mathbf{w}, \mathbf{v}), \mathbf{v} + \mathbf{p}(\mathbf{v}))] \tag{29}$$

and

$$\tilde{f}_2 = f_2(\mathbf{w} + \mathbf{H}(\mathbf{w}, \mathbf{v}), \mathbf{h}(\mathbf{w}, \mathbf{v}), \mathbf{v} + \mathbf{p}(\mathbf{w})) - D\mathbf{h}(\mathbf{w}, \mathbf{v})\mathbf{C}(\mathbf{w}, \mathbf{v}) + T(\mathbf{w}, \mathbf{v})D\mathbf{h}(\mathbf{w}, \mathbf{v})[I + D\mathbf{H}(\mathbf{w}, \mathbf{v})]^{-1} \times [J_0(\mathbf{w} + \mathbf{H}(\mathbf{w}, \mathbf{v})) + f_1(\mathbf{w} + \mathbf{H}(\mathbf{w}, \mathbf{v}), \mathbf{h}(\mathbf{w}, \mathbf{v}), \mathbf{v} + \mathbf{p}(\mathbf{v}))], \tag{30}$$

respectively. Note that  $\tilde{f}_1$  and  $\tilde{f}_2$  contain  $T_m$  and  $\mathbf{p}_m$ .

Now we can determine the  $m$ th order normal form coefficients  $\mathbf{C}_m$ , and the nonlinear transformation coefficients  $\mathbf{H}_m$  and  $\mathbf{h}_m$  as well as the rescalings  $T_m$  and  $\mathbf{p}_m$  from Eq. (28) order by order starting from  $m = 2$ . Firstly, note from Eq. (23) that the  $m$ th order coefficients  $\tilde{f}_{1m}$  and  $\tilde{f}_{2m}$  contain  $\mathbf{C}$ ,  $\mathbf{H}$ ,  $\mathbf{h}$ ,  $T$  and  $\mathbf{p}$  coefficients whose orders are lower than  $m$ . Therefore, the undetermined lower order coefficients may be involved in the two coefficients  $\tilde{f}_{1m}$  and  $\tilde{f}_{2m}$ . Secondly, since  $\lambda_0$  only contains the eigenvalues of  $J_0$  (with zero real parts) and all eigenvalues of  $J_1$  have non-zero real parts,  $\lambda_0 I - J_1$  cannot equal zero for any of its components. This suggests that  $\mathbf{h}_m$  can be uniquely determined from Eq. (28) as

$$\mathbf{h}_m = [\lambda_0 I - J_1]^{-1} \tilde{f}_{2m}, \tag{31}$$

or, by noting that  $[\lambda_0 I - J_1]$  is a diagonal matrix,

$$h_m^{(k)} = \frac{\tilde{f}_{2m}^{(k)}}{\lambda_0 - \lambda_{n_0+k}} \quad (k = 1, 2, \dots, n - n_0), \tag{32}$$

where  $h_m^{(k)}$  and  $\tilde{f}_{2m}^{(k)}$  are the  $k$ th components of  $\mathbf{h}_m$  and  $\tilde{f}_{2m}$ , respectively.

Finally, we need to solve the equation:

$$[\lambda_0 I - J_0]\mathbf{H}_m = \tilde{f}_{1m} - \mathbf{C}_m \tag{33}$$

to determine  $\mathbf{C}_m$  and  $\mathbf{H}_m$ . Note that  $\tilde{f}_{1m}$  contains the lower order coefficients of  $\mathbf{C}$ ,  $\mathbf{H}$ ,  $T$  and  $\mathbf{p}$ , and thus unlike the CNF computation, we may use the lower order  $\mathbf{H}$ ,  $\mathbf{h}$ ,  $T$  and  $\mathbf{p}$  coefficients to eliminate  $\mathbf{C}_m$ , leading to the SNF. Similarly, due to the semi-simple property, the matrix  $[\lambda_0 I - J_0]$  is a diagonal matrix, one can rewrite Eq. (33) in the component form:

$$(\lambda_0 - \lambda_k)H_m^{(k)} = \tilde{f}_{1m}^{(k)} - C_m^{(k)} \quad (k = 1, 2, \dots, n_0), \tag{34}$$

where  $H_m^{(k)}$ ,  $\tilde{f}_{1m}^{(k)}$  and  $C_m^{(k)}$  are the  $k$ th components of  $\mathbf{H}_m$ ,  $\tilde{f}_{1m}$  and  $\mathbf{C}_m$ , respectively. Then when  $\lambda_0 - \lambda_k \neq 0$ , we may uniquely determine

$$C_m^{(k)} = 0 \quad \text{and} \quad H_m^{(k)} = \frac{\tilde{f}_{1m}^{(k)}}{\lambda_0 - \lambda_k}. \tag{35}$$

However, when  $\lambda_0 - \lambda_k = 0$ , we may use the lower order  $\mathbf{H}$ ,  $\mathbf{h}$ ,  $T$  and  $\mathbf{p}$  coefficients involved in  $\tilde{f}_{1m}$  to possibly eliminate  $C_m^{(k)}$ . If there are no such lower order coefficients which can be used at this order, then  $C_m^{(k)} = \tilde{f}_{1m}^{(k)}$ . The rule determining how to choose the lower order coefficients depends upon the singularity under consideration.

Having found the explicit formulas (32) and (34), it seems that the computation of the coefficients of the normal form and nonlinear transformation is straightforward. However, it has been noted that directly employing these formulas can cause computation problem: A computer may quickly run out of its memory due to enormous algebraic manipulations. As we know that in the computation of normal forms, higher order computations do not affect lower order results, but lower order results influence all higher order calculations. In general, when one finishes  $k < m$  order computations, one substitutes the lower order solutions into the original nonlinear function  $\mathbf{f}$  to obtain the equation for computing the  $m$ th order normal form. The expression of the resulting equation includes all order ( $< m$  and  $\geq m$ ) expressions and one needs to extract the exact  $m$ th order part from the enormous large expression. In fact, the semi-simple case has been considered with the ‘‘extract’’ method. It has been found that such an approach is not efficient and can easily cause a computer ‘‘crash’’ even for a not very complicated problem. In order to overcome this difficulty, it needs to directly find the expression which only belongs to the  $m$ th order equation. This can greatly reduce the computation time and computer memory demanding. The detailed efficient computation approach will not be discussed in this paper. Interested readers are referred to Refs. [22–26].

### 3. The SNF for codimension-one singularity

In the previous section, we have developed an efficient computation method and derived recursive formulas for computing the coefficients of the SNF and associated transformations (see Eqs. (31) and (34)). It has been shown that the transformation for the non-critical variables,  $\mathbf{h}$ , is uniquely determined by Eq. (31). However, computing the center manifold part is not straightforward. (The computation of this part for the CNF is straightforward, uniquely determined by Eq. (33), see [23].) To find the SNF from Eq. (34) one must carefully consider not only the coefficients of  $\mathbf{H}$ , but also that of  $T$  and  $\mathbf{p}$  which are implicitly involved in  $\tilde{\mathbf{f}}_1$ . It should be emphasized that Eq. (34) does not contain  $\mathbf{h}$  coefficients since the  $k$ th order coefficients  $\mathbf{h}_k$  are solved and only solved from the  $k$ th order algebraic Eq. (31). This implies that Eq. (34) only contains  $\mathbf{H}$ ,  $T$  and  $\mathbf{p}$  which are associated with the center manifold variables,  $\mathbf{u}$  and  $\mathbf{v}$ . Therefore, the final step in computing the SNF is to solve Eq. (34), which is similar to finding the SNF of a system which is described on center manifold. However, we cannot obtain a general form or procedure applicable for all semi-simple cases. One has to deal with the singularities case by case. In this paper, we focus on codimension-one singularities: single zero and Hopf bifurcation. The SNF for the two singularities based on center manifold (i.e., the original system (3) is not a general  $n$ -dimensional system, but described on center manifold) have been obtained in [22,29]. Therefore, in the following we will outline the computation rules of the SNF for the two singularities.

#### 3.1. The SNF for single zero

As discussed above, to find the computation rules of the SNF of single zero singularity, we may assume that the original system is described on one-dimensional center manifold as follows:

$$\frac{dy}{dt} = f(y, \mu) = \sum_{i=1}^{\infty} a_{1i} \mu^i y + \sum_{i=0}^{\infty} a_{2i} \mu^i y^2 + \sum_{i=0}^{\infty} a_{3i} \mu^i y^3 + \dots \tag{36}$$

which has an equilibrium  $x = 0$  for any real values of  $\mu$ . The near-identity nonlinear transformation and the time scaling are, respectively, given by

$$y = w + H(w, \mu) = w + \sum_{i=1}^{\infty} b_{1i} \mu^i w + \sum_{i=0}^{\infty} b_{2i} \mu^i w^2 + \dots \tag{37}$$

and

$$T_0 + T(w, \mu) = 1 + \sum_{i=1}^{\infty} T_{0i} \mu^i + \sum_{i=0}^{\infty} T_{1i} \mu^i w + \sum_{i=0}^{\infty} T_{3i} \mu^i w^2 + \dots \tag{38}$$

It has been shown [22] that the case of zero singularity does not need parameter scaling (reparametrization). Thus, instead of  $v$ , the original parameter  $\mu$  is used in Eqs. (37) and (38).

It has been proved [22] that under the conditions:

$$a_{11} \neq 0 \quad \text{and} \quad a_{k0} \neq 0 \quad (k \geq 2), \tag{39}$$

where  $a_{k0}$  is the first non-zero coefficients of  $a_{j0}$ 's, the SNF of system (36) is given by

$$\frac{dw}{d\tau} = a_{11} \mu w + a_{k0} w^k \quad (k \geq 2), \tag{40}$$

up to any order.

Note that the coefficients  $a_{11}$  (for the 2nd order equation) and  $a_{k0}$  (for the  $k$ th order equation) are known coefficients of the original system, indicating that the 2nd order equation cannot be reduced. The detailed procedure for computing the coefficients of  $b_{ij}$  and  $T_{ij}$  can be found in [22]. The above results are based on the assumption  $a_{11} \neq 0$ , which results in the unfolding  $a_{11} \mu w$ . Other possible unfolding may not be so simple if  $a_{11} = 0$ . However, they can be easily obtained by executing the Maple program we developed to find the SNF. For example, suppose  $a_{11} = a_{12} = 0$ , but  $a_{13} \neq 0$  and  $a_{21} \neq 0$ , then the SNF is found to be

$$\frac{dw}{d\tau} = a_{13} \mu^3 w + a_{21} \mu w^2 + a_{k0} w^k \quad (k \geq 2). \tag{41}$$

The above rules obtained based on center manifold can be applied to solve the key Eq. (34) for the general original system (3). However, it should be noted that the coefficient  $a_{k0}$  cannot be directly observed from the original equation (e.g., usually the first equation of the system) since non-center manifold equations may have contributions to these coefficients. This can be easily handled in symbolic computation.

3.2. *The SNF for Hopf bifurcation*

We now turn to Hopf bifurcation. Again, we first discuss the system given on a 2-dimensional center manifold to find the rules of computing the coefficients of the SNF and transformations. Suppose the system is described in complex form:

$$\frac{dz}{dt} = \begin{bmatrix} i & 0 \\ 0 & -i \end{bmatrix} z + f(z, \mu) \equiv \begin{bmatrix} i & 0 \\ 0 & -i \end{bmatrix} \begin{pmatrix} z \\ \bar{z} \end{pmatrix} + \begin{pmatrix} f(z, \bar{z}, \mu) \\ \bar{f}(z, \bar{z}, \mu) \end{pmatrix}, \tag{42}$$

where  $z = (z, \bar{z})^T$  and  $f = (f, \bar{f})^T$ ,  $T$  represents transpose.  $\bar{z}$  and  $\bar{f}$  are complex conjugates of  $z$  and  $f$ , respectively.

Further, assume that

$$\begin{aligned} f_k &= \sum_{j+l+m=k} (a_{1jlm} + ia_{2jlm}) z^j \bar{z}^l \mu^m, \\ H_k &= \sum_{j+l+m=k} (b_{1jlm} + ib_{2jlm}) w^j \bar{w}^l v^m, \\ C_2 &= [(\alpha_1 + i\beta_1)w + (\alpha_2 + i\beta_2)\bar{w}]v, \\ C_k &= (c_{1k} + ic_{2k})w^{(k+1)/2}\bar{w}^{(k-1)/2} \quad (k \geq 3, \text{ odd integer}), \\ t &= (T_0 + T(w, \bar{w}, v))\tau \left( 1 + \sum_{k=1} \sum_{j+m=k} t_{jm} \left[ \frac{1}{2}(w + \bar{w}) \right]^j v^m \right) \tau, \\ \mu &= p_0v + p(v) = v + \sum_{j=2} p_j v^j, \end{aligned} \tag{43}$$

where  $C_2$  represents the linear unfolding.

Applying the 2nd-order ( $k = 2$ ) equations of (34) yields the following solutions:

$$\begin{aligned} b_{1200} &= a_{2200}, & b_{2200} &= -a_{12001}, & b_{1020} &= -\frac{1}{3}a_{2020}, \\ b_{2020} &= \frac{1}{3}a_{1020}, & b_{1110} &= -a_{2110}, & b_{2110} &= a_{1110}, \end{aligned} \tag{44}$$

and

$$\begin{aligned} \alpha_1 &= a_{1101}, & t_{01} &= -a_{2101}, \\ b_{1011} &= -\frac{1}{2}a_{2011}, & b_{2011} &= \frac{1}{2}a_{1011}, \end{aligned} \tag{45}$$

which results in

$$\beta_1 = \alpha_2 = \beta_2 = 0. \tag{46}$$

Next, for  $k = 3$ , similarly we can find the following solutions:

$$\begin{aligned} c_{13} &= a_{1210} - A_{1210}, \\ t_{20} &= 2(b_{23} - a_{2210} + A_{2210}), \\ p_2 &= -\frac{1}{a_{1101}}(a_{1102} + A_{1102}), \\ t_{02} &= \frac{a_{2101}}{a_{1101}}(a_{1102} + A_{1102}) - (a_{2102} + A_{2102}), \\ b_{2300} &= -\frac{1}{2}(a_{1300} + A_{1300}), \\ b_{1300} &= \frac{1}{2} \left( a_{2300} + A_{2300} + \frac{1}{4}t_{20} \right), \\ b_{2030} &= \frac{1}{4}(a_{1030} - A_{1030}), \end{aligned}$$



$$\begin{aligned}
 b_{1030} &= -\frac{1}{4}(a_{2030} - A_{2030}) \\
 b_{2120} &= \frac{1}{2}(a_{1120} - A_{1120}), \\
 b_{1120} &= -\frac{1}{2}\left(a_{2120} - A_{2120} + \frac{1}{4}t_{20}\right), \\
 b_{2201} &= -(a_{1201} + A_{1201}), \\
 b_{1201} &= a_{2201} + A_{2201}, \\
 b_{2021} &= \frac{1}{3}(a_{1021} - A_{1021}), \\
 b_{1021} &= -\frac{1}{3}(a_{2021} - A_{2021}), \\
 b_{2111} &= a_{1111} - A_{1111}, \\
 b_{1111} &= -(a_{2111} - A_{2111}), \\
 b_{2012} &= \frac{1}{2}(a_{1012} - A_{1012} + p_2 a_{1011}), \\
 b_{1012} &= -\frac{1}{2}(a_{2012} - A_{2012} + p_2 a_{2011}), \\
 b_{1101} &= c_{2101} = t_{11} = 0,
 \end{aligned} \tag{47}$$

where  $A_{jkl}$ 's are known expressions, given in terms of  $a_{ijlm}$ 's. We can apply the above procedure to solve higher order equations using the general rules given in [29]. Note that most of the equations are uniquely solved using the coefficients  $b_{ijlm}$ .

Therefore, the complex SNF of Hopf bifurcation is given by

$$\frac{dw}{d\tau} = iw + a_{1101}wv + (a_{1210} - a_{1200}a_{2110} - a_{2200}a_{1110})w^2\bar{w} + i \sum_{m=1}^{\infty} c_{2(2m+1)}w^{m+1}\bar{w}^m, \tag{48}$$

where  $c_{2j}$  are explicitly obtained in terms of the original system coefficients  $a_{ijlm}$ 's.

Letting  $w = Re^{i\theta}$ , where  $R$  and  $\theta$  are, respectively, the amplitude and phase of motion, and splitting the real and imaginary parts in Eq. (48) results in the equations, given in polar coordinates:

$$\frac{dR}{d\tau} = a_{1101}vR + (a_{1210} - a_{1200}a_{2110} - a_{2200}a_{1110})R^3, \tag{49}$$

$$\frac{d\theta}{d\tau} = 1 + c_{23}R^2 + c_{25}R^4 + \dots + c_{2(2m+1)}R^{2m} + \dots \tag{50}$$

Note that when we derive the SNF of Hopf bifurcation it has been assumed  $a_{1101} \neq 0$ . This is clear from Eq. (49) that no linear universal unfolding will be present if  $a_{1101} = 0$ . The bifurcation and stability analysis can be carried out using Eq. (49). The steady-state solutions are given by

$$\begin{aligned}
 \text{(I)} \quad &R = 0, \\
 \text{(II)} \quad &R^2 = -\frac{a_{1101}v}{a_{1210} - a_{1200}a_{2110} - a_{2200}a_{1110}},
 \end{aligned} \tag{51}$$

where solution (I) actually represents the original equilibrium, while solution (II) denotes a family of limit cycles. The stability of the steady-state solutions can be easily determined as follows: solution (I) is stable (unstable) if  $a_{1101}v < 0$  ( $> 0$ ). Solution (II) is stable (unstable) if  $S_{LC} \equiv a_{1210} - a_{1200}a_{2110} - a_{2200}a_{1110} < 0$  ( $> 0$ ). If  $S_{LC} < 0$ , then the existence of the limit cycles for  $a_{1101}v > 0$  implies that the original equilibrium and the periodic solution exchange their stabilities at the critical point  $v = 0$ . This is called supercritical Hopf bifurcation. Otherwise, it is called subcritical Hopf bifurcation.

The above analysis seems like a typical Hopf bifurcation analysis using the CNF. However, it should be noted that all higher order terms ( $> 3$ ) have been removed from the SNF while the CNF has infinitely many higher order terms.

Thus, Hopf bifurcation analysis based on the CNF up to 3rd-order terms means that all higher order terms in the CNF are neglected. For the SNF, however, the exact 3rd-degree polynomial is used for the analysis.

The above procedure can be directly applied to the general original  $n$ -dimensional system (3). Symbolic program has been coded using Maple.

#### 4. Applications

In this section, we shall present two examples to demonstrate how to use the results obtained in the previous sections to consider feedback control on bifurcations associated with single zero and Hopf singularities. The first example is the well-known Lorenz system and the second one is a nonlinear electrical circuit.

##### 4.1. The Lorenz system

The Lorenz system is given by [2]

$$\begin{aligned}\frac{dx}{dt} &= -p(x-y), \\ \frac{dy}{dt} &= -xz-y, \\ \frac{dz}{dt} &= xy-z-r,\end{aligned}\tag{52}$$

where  $p$  and  $r$  are positive parameters, considered as control parameters. Note that system (52) is a special case of the standard Lorenz equation (e.g., see [30]):

$$\begin{aligned}\frac{dx}{dt} &= -\sigma(x-y), \\ \frac{dy}{dt} &= \rho x - xz - y, \\ \frac{dz}{dt} &= xy - \beta z,\end{aligned}\tag{53}$$

which has one more parameter than system (52). One can easily show that system (52) is a special case of system (53) by first setting  $\beta = 1$  in Eq. (53). Then let  $p = \sigma$  and  $r = \rho$ , and use a constant shift  $z = \tilde{z} - r$  in system (53) to obtain the standard Lorenz Eq. (52) for  $\beta = 1$ .

It can be shown that system (52) has three equilibrium solutions  $C_0$ ,  $C_+$  and  $C_-$ , given by

$$\begin{aligned}C_0 : x_e = y_e = 0, \quad z_e = -r, \\ C_{\pm} : x_e^{\pm} = y_e^{\pm} = \pm\sqrt{r-1}, \quad z_e^{\pm} = -1.\end{aligned}\tag{54}$$

Suppose the parameters  $p$  and  $r$  are positive, then  $C_0$  is stable for  $0 \leq r < 1$ , and a pitchfork bifurcation occurs at  $r = 1$ , where equilibrium solution  $C_0$  bifurcates into either  $C_+$  or  $C_-$ . The two equilibria  $C_+$  and  $C_-$  are stable for  $1 < r < r_H$ , where

$$r_H = \frac{p(p+4)}{p-2} \quad (p > 2)\tag{55}$$

indicates a critical point at which  $C_+$  and  $C_-$  lose their stabilities, giving rise to Hopf bifurcation. To have  $r_H = 16$  which is used in [2], it follows from Eq. (55) that  $p = 4$  or  $8$ . Since the value of  $p = 4$  has been used in [2], we choose  $p = 8$  in this paper.

In the following, we will consider two singularities of system (52): single zero and Hopf bifurcation. Although for the zero case it is easy to find the stabilities of the equilibrium solutions from the original system (52), one cannot find the post-critical bifurcation solutions as well as bifurcation equations directly from Eq. (52), but may obtain the bifurcation equation using normal form theory.

##### 4.1.1. Single zero

First consider single zero singularity and start from equilibrium  $C_0$ . Let

$$z = -r + \tilde{z} \quad \text{and} \quad r = r_c + \mu \equiv 1 + \mu,\tag{56}$$

where  $\mu$  is a perturbation parameter. Substituting Eq. (56) into (52) yields

$$\begin{aligned} \frac{dx}{dt} &= \left(\frac{4}{5}x - \frac{16}{5}\tilde{z}\right)\mu - \frac{4}{5}xy + \frac{16}{5}y\tilde{z}, \\ \frac{dy}{dt} &= -y + x^2 - 3x\tilde{z} - 4\tilde{z}^2, \\ \frac{d\tilde{z}}{dt} &= -5\tilde{z} + \left(\frac{1}{5}x - \frac{4}{5}\tilde{z}\right)\mu - \frac{1}{5}xy + \frac{4}{5}y\tilde{x}. \end{aligned} \tag{57}$$

At the critical point:  $r_c = 1$ , the Jacobian of system (57) evaluated at the equilibrium  $x = y = \tilde{z} = 0$  has one zero and two negative eigenvalues, 0,  $-1$  and  $-9$ . Now applying the Maple program developed in this paper yields the following SNF:

$$\frac{dw}{dt} = \frac{4}{5}w(\mu - w^2). \tag{58}$$

The near-identity transformation and time rescaling can be obtained up to an arbitrary order. For example, the results up to 5th order are given as follows: The near-identity transformation is

$$\begin{aligned} x &= w - \left(\frac{906}{625}\mu^2 + \frac{566586}{15625}\mu^3 + \frac{84814353}{78125}\mu^4\right)w + \frac{906}{625}w^5, \\ y &= w^2 - \left(\frac{43}{25}\mu + \frac{72}{625}\mu^2 + \frac{1117736}{15625}\mu^3\right)w^2 + \left(\frac{43}{25} - \frac{5353}{625}\mu\right)w^4, \\ \tilde{z} &= \left(\frac{1}{25}\mu - \frac{8}{625}\mu^2 - \frac{842}{15625}\mu^3 - \frac{2795626}{1953125}\mu^4\right)w - \left(\frac{1}{25} - \frac{67}{625}\mu - \frac{66}{3125}\mu^2\right)w^3 - \frac{59}{625}w^5, \end{aligned} \tag{59}$$

and the time scaling is given by

$$\begin{aligned} T &= \frac{4}{25}\mu - \frac{94}{25}w^2 - \frac{32}{625}\mu^2 - \frac{16}{625}w^2\mu + \frac{128}{15625}\mu^3 - \frac{2240144}{15625}w^2\mu^2 + \frac{26432}{1953125}\mu^4 \\ &\quad - \frac{7949170916}{1953125}w^2\mu^3 + \frac{18372928}{48828125}\mu^5. \end{aligned} \tag{60}$$

Note that the last two equations given in Eq. (59) represent the transformation between the center manifold and the non-critical variables.

The governing Eq. (58) is a typical pitchfork bifurcation. Eq. (58) has three equilibrium solutions:  $w = 0$  and  $w = \pm\sqrt{\mu}$  ( $\mu \geq 0$ ). The former is the original equilibrium solution  $x = y = 0, z = -r$ , which is stable when  $\mu < 0$  (i.e.,  $r < 1$ ), while the latter is the post-critical bifurcation solution which is stable for  $\mu > 0$  (i.e.,  $r > 1$ ). The bifurcation solution is actually the approximation of the original equilibrium solutions  $C_{\pm}$  in the vicinity of the critical point,  $\mu = 0$ . Therefore, the bifurcation diagram, shown in Fig. 1(a), suggests that the equilibrium solution  $C_0$  bifurcates into equilibrium solutions  $C_{\pm}$  at the critical point  $r = 1$  (or vice verser) and exchange their stabilities. The numerical simulation result for  $\mu = 0.5$  (or  $r = 1.5$ ) is depicted in Fig. 1(b).

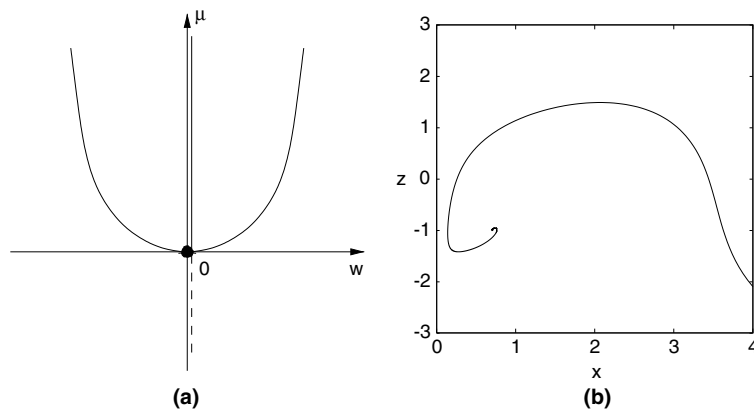


Fig. 1. Single zero singularity of the Lorenz equation (61): (a) bifurcation diagram; and (b) numerical simulation of bifurcation solution for  $r = 1.5$  with the initial condition  $(x, y, z) = (4.0, 3.1, -2.1)$ .

4.1.2. Hopf bifurcation

Now we turn to consider Hopf bifurcation which plays an important role in studying limit cycles. It is well known that the Lorenz system (52) can exhibit subcritical Hopf bifurcation arising from the equilibrium  $C_+$  or  $C_-$ . Also it is well known that the Lorenz system can have chaotic motion for certain parameter values. In fact, system (52) can have chaos when  $r = 14$ . In the past two decades, there has been rapidly growing interest in controlling and anti-controlling bifurcations and chaos (e.g., see [2,3]). There are a wide variety of promising potential applications of bifurcation and chaos control. In general, the aim of bifurcation control is to design a controller such that the bifurcation characteristics of a nonlinear system undergoing bifurcation can be modified to achieve some desirable dynamical behavior, such as changing a Hopf bifurcation solution from subcritical to supercritical, eliminating chaotic motions, etc. In the following, we will use the SNF obtained in the previous sections to show how to design a control system such that unstable limit cycles become stable. First, we consider system (52) without control and then study a feedback control applied to system (52).

**Without control.** For this case, the critical point at which Hopf bifurcation occurs is defined by Eq. (56). At the critical point the Jacobian of system (52) evaluated at  $C_+$  has a real eigenvalue  $-10$  and a purely imaginary pair  $\pm 2\sqrt{6}$ . Using a translation, given by

$$x = \sqrt{r-1} + \tilde{x}, \quad y = \sqrt{r-1} + \tilde{y}, \quad z = -1 + \tilde{z}, \tag{61}$$

we move  $C_+$  to the origin and then apply an appropriate linear transformation to system (52) to find the following system:

$$\begin{aligned} \frac{d\tilde{x}}{dt} &= 2\sqrt{6}\tilde{y} + \left( \frac{17}{310}\tilde{x} + \frac{19\sqrt{6}}{310}\tilde{y} - \frac{39}{155}\tilde{z} \right)\mu + \frac{344}{7595}\tilde{x}^2 + \frac{2736}{7595}\tilde{y}^2 \\ &\quad - \frac{432}{155}\tilde{z}^2 + \frac{866\sqrt{6}}{7595}\tilde{x}\tilde{y} - \frac{228}{1085}\tilde{x}\tilde{z} - \frac{696\sqrt{6}}{1085}\tilde{y}\tilde{z} + \dots, \\ \frac{d\tilde{y}}{dt} &= -2\sqrt{6}\tilde{x} - \left( \frac{29\sqrt{6}}{465}\tilde{x} + \frac{1}{155}\tilde{y} + \frac{53\sqrt{6}}{930}\tilde{z} \right)\mu - \frac{1072\sqrt{6}}{7595}\tilde{x}^2 \\ &\quad - \frac{48\sqrt{6}}{7595}\tilde{y}^2 + \frac{236\sqrt{6}}{155}\tilde{z}^2 - \frac{4888}{7595}\tilde{x}\tilde{y} + \frac{4352\sqrt{6}}{3255}\tilde{x}\tilde{z} - \frac{612}{1085}\tilde{y}\tilde{z} + \dots, \\ \frac{d\tilde{z}}{dt} &= -10\tilde{z} - \left( \frac{2}{93}\tilde{x} - \frac{\sqrt{6}}{186}\tilde{y} + \frac{3}{62}\tilde{z} \right)\mu - \frac{256}{4557}\tilde{x}^2 + \frac{48}{1519}\tilde{y}^2 \\ &\quad + \frac{12}{31}\tilde{z}^2 - \frac{160\sqrt{6}}{4557}\tilde{x}\tilde{y} + \frac{120}{217}\tilde{x}\tilde{z} - \frac{22\sqrt{6}}{217}\tilde{y}\tilde{z} + \dots, \end{aligned} \tag{62}$$

where  $\mu = r - 16$  and  $\dots$  represents higher order terms.

Employing the Maple programs developed for computing the SNF of Hopf bifurcation yields the SNF:

$$\frac{dR}{d\tau} = R \left( \frac{3}{124}v + \frac{139}{53165}R^2 \right), \tag{63}$$

$$\begin{aligned} \frac{d\Theta}{d\tau} &= 2\sqrt{6} \left[ 1 + \frac{23}{744}v - \frac{3281317933639}{319247852376600}R^2 - \left( \frac{26339292381157493078902472268437}{166438490308647816971712788230471875} \right. \right. \\ &\quad \left. \left. - \frac{6627347639944444075371091284247\sqrt{6}}{60523087384962842535168286629262500} \right) R^4 + \dots \right]. \end{aligned} \tag{64}$$

The near-identity transformation, time scaling and parameter rescaling are also obtained. The time scaling and parameter rescaling are given:

$$\begin{aligned} \mu = v &+ \frac{61}{3844}v^2 - \frac{2361289}{10638961920}v^3 + \frac{854409017}{79153876684800}v^4 \\ &- \left( \frac{1050588067437389}{3395625322056302592000} + \frac{1948975\sqrt{6}}{441678631901184} \right) v^5 + \dots, \end{aligned} \tag{65}$$

$$\begin{aligned}
 T = & \frac{245}{2214144} v^2 - \frac{771331822487}{79811963094150} w^2 - \frac{143045}{25533508608} v^3 + \frac{293860231}{3140825826852864} v^4 \\
 & - \left( \frac{9258883163330958269601609110008247}{15978095069630190429284427670125300000} + \frac{13254695279888888150742182568494\sqrt{6}}{45392315538722131901376214971946875} \right) w^4 \\
 & + \left( \frac{908362417529}{651960061834810097664} + \frac{2321767\sqrt{6}}{21200574331256832} \right) v^5 + \dots, \tag{66}
 \end{aligned}$$

where  $w = R \cos \Theta$ . The lengthy near-identity transformation is omitted.

It is easy to see from the first equation of (64) that the Hopf bifurcation is subcritical. Next, we shall apply a feedback control to system (52) such that the Hopf bifurcation becomes supercritical.

**With control.** The control of Hopf bifurcation of Lorenz system (52) has been considered in [2], where a feedback control  $u$ , utilizing a washout filter, was proposed to obtain

$$\begin{aligned}
 \frac{dx}{dt} &= -p(x - y), \\
 \frac{dy}{dt} &= -xz - y, \\
 \frac{dz}{dt} &= xy - z - r - u, \\
 \frac{dv}{dt} &= y - cv,
 \end{aligned} \tag{67}$$

where  $v$  is the state of the washout filter used for control:

$$u = -k_c(y - cv) - k_n(y - cv)^3, \tag{68}$$

with constant gains  $k_c$  and  $k_n$ , and  $c$  is a constant chosen for the filter. Note in Eq. (68) that we use negative sign for  $u$  while positive sign is used in [2], where the numerical results showed that with  $c = 0.5$ ,  $k_c = 2.5$ ,  $k_n = 0.009$  and  $p = 4$ , the critical value  $r_H$  is increased from 16 to about 36, and the limit cycles bifurcating from  $C_+$  are unstable.

We shall now present an analytical approach to study the controlled system (67) for  $p = 8$ . First it is easy to show that the system still have three equilibrium solutions:

$$\begin{aligned}
 C_0 : x_e = y_e = 0, \quad z_e = -r, \quad v_e = 0, \\
 C_{\pm} : x_e^{\pm} = y_e^{\pm} = \pm\sqrt{r-1}, \quad z_e^{\pm} = -1, \quad v_e^{\pm} = \pm\frac{1}{c}\sqrt{r-1}.
 \end{aligned} \tag{69}$$

Comparing Eq. (69) with Eq. (55) indicates that the controlled system (55) keeps the equilibria of the original system (52) unchanged, showing the advantage of introducing the washout filter. By a linear analysis with the aid of Hurwitz criterion, one can easily find that when  $c = 0.5$  and  $k_c = 2.5$  ( $k_n$  does not affect linear stability), the equilibrium  $C_+$  is stable for  $1 < r < r_H = 22.59470931$  while the  $C_-$  is stable for  $1 < r < r_H = 1.06728042$ . This suggests that, by noting that both the two equilibria  $C_{\pm}$  of the original system are (locally) stable for  $1 < r < r_H = 16$ , the feedback control (68) is beneficial for the stability of the  $C_+$  since it receives 41.2% increase of stable interval over the original one. However, it dramatically decreases the stability of the  $C_-$  with almost zero stable interval, indicating that this control strategy is not good for simultaneously controlling the two Hopf bifurcations for  $C_{\pm}$ . A better alternative control approach has been proposed in [6], and later extended to consider difference equations [7] and time delay systems [8]. This approach will be used in the next example.

Let us consider  $C_+$  first. Similarly, we can shift  $C_+$  to the origin, at which the Jacobian of the system evaluated at the critical point  $r_H = 22.59470931$  has four eigenvalues: One purely imaginary pair:  $\pm 6.57377850i$  and two negative real eigenvalues:  $-0.39563830$  and  $-10.10436170$ . We can apply a linear transformation to change system (67) into the following form:

$$\begin{aligned}
 \frac{d\tilde{x}}{dt} &= 6.57377850\tilde{y} - (0.00236833\tilde{x} - 0.10407365\tilde{y} + 0.01129543\tilde{z} + 0.06367725\tilde{v})\mu + \dots, \\
 \frac{d\tilde{y}}{dt} &= -6.57377850\tilde{x} - (0.14454189\tilde{x} - 0.04039567\tilde{y} - 0.01615943\tilde{z} - 0.02193977\tilde{v})\mu + \dots, \\
 \frac{d\tilde{z}}{dt} &= -0.39563830\tilde{z} + (0.01049911\tilde{x} + 0.00396952\tilde{y} - 0.00194553\tilde{z} - 0.00586872\tilde{v})\mu + \dots, \\
 \frac{d\tilde{v}}{dt} &= -10.1043617\tilde{v} + (0.00980539\tilde{x} - 0.06341171\tilde{y} + 0.00568612\tilde{z} + 0.03608181\tilde{v})\mu + \dots,
 \end{aligned} \tag{70}$$

where  $\dots$  denote higher degree homogeneous polynomials of  $\tilde{x}, \tilde{y}, \tilde{z}, \tilde{v}$  and  $\mu$ . Applying the Maple program yields the following SNF:

$$\begin{aligned} \frac{dR}{d\tau} &= R[0.01901367v - (0.02031627k_n - 0.00313739)R^2], \\ \frac{d\Theta}{d\tau} &= 6.57377850 + \frac{0.29963407k_n^2 - 0.04676775k_n + 0.00975412}{k_n - 0.15442729}R^2 + \dots \end{aligned} \tag{71}$$

A similar analysis on the equilibrium point  $C_-$  leads to the following SNF:

$$\begin{aligned} \frac{dR}{d\tau} &= R[1.04131271v - (0.42622679 - 0.00711275k_n)R^2], \\ \frac{d\Theta}{d\tau} &= 0.20057843 + \frac{0.00445422k_n^2 - 0.21102439k_n + 78.87634463}{k_n - 59.92429033}R^2 + \dots \end{aligned} \tag{72}$$

It follows from the first equations of (71) and (72) that the Hopf bifurcation from the  $C_+$  is supercritical when

$$\left. \begin{aligned} 0.02031627k_n - 0.00313739 > 0 \\ k_n - 0.15442729 \neq 0 \end{aligned} \right\} \text{ i.e., } k_n > 0.15442730, \tag{73}$$

while that from the  $C_-$  is supercritical if

$$\left. \begin{aligned} 0.42622679 - 0.00711275k_n > 0 \\ k_n - 59.92429033 \neq 0 \end{aligned} \right\} \text{ i.e., } k_n < 59.92429032. \tag{74}$$

In order for both the Hopf bifurcations emerging from  $C_+$  and  $C_-$  to be supercritical, it requires that

$$0.15442730 < k_n < 59.92429032. \tag{75}$$

In other words, when the control parameters  $c, k_c$  and  $k_n$  are taken as  $c = 0.5, k_c = 2.5$  and  $k_n \in (0.15442730, 59.92429032)$ , all the limit cycles bifurcating either from  $C_+$  or  $C_-$  become stable. When the values of  $c$  and  $k_c$  are varied, the interval for  $k_n$  is changed, and the new values of  $k_n$  can be found using the above procedure. This becomes quite easy by using the Maple program. It should be noted however that since the Hopf critical point on  $C_-$  is  $r_H = 1.06728042$  which is very close to the static bifurcation point  $r_c = 1$  at which  $C_+$  and  $C_-$  bifurcate from the  $C_0$ , the equilibrium  $C_-$  almost does not exist.

Some numerical simulation results are given in Figs. 2–4, which are the projections of the trajectories from the 4-dimensional space  $(x, y, z, v)$  into the 2-dimensional space  $(x, z)$ . Fig. 2 shows the trajectories of the controlled system (67) for  $p = 8, c = 0.5, k_c = 2.5$  and  $k_n = 0.009$ . It is seen from Fig. 2(a) that when  $r = 20 \in (1, 22.59470931)$ , the trajectory converges to the equilibrium  $C_+$  even for an initial point not near the  $C_+$ . When  $r = 23.5 > r_H = 22.59470931$ , the bifurcating limit cycle is unstable and diverges to a chaotic attractor (see Fig. 2(b)).

Fig. 3 shows the numerical simulation results when  $p = 8, c = 0.5, k_c = 2.5$  (which are same as that for Fig. 2), but  $k_n = 10 \in (0.15442730, 59.92429032)$ . It is observed that the periodic solutions bifurcating from  $C_+$  for  $r > r_H = 22.59470931$  are all stable. For the values of  $r$  close to  $r_H$  (see Fig. 3(a) in which  $r = 24$ , the bifurcating limit

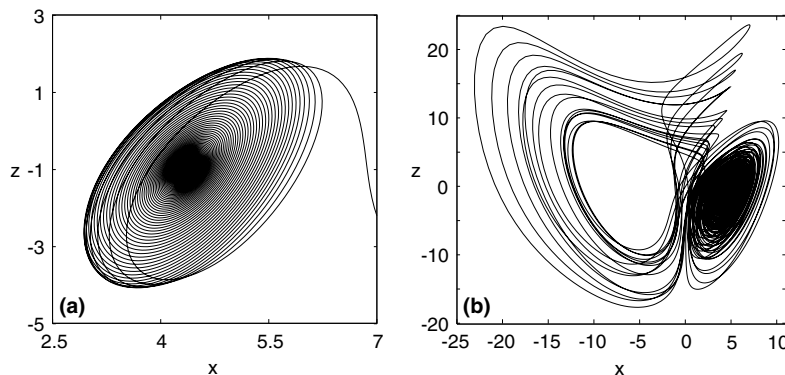


Fig. 2. Trajectories of the controlled Lorenz system (64) for  $p = 8, c = 0.5, k_c = 2.5$  and  $k_n = 0.009$ : (a) convergent to  $C_+$  when  $r = 20$  with  $(x_0, y_0, z_0, v_0) = (8, 5, -4.0, 15)$ ; and (b) divergent to a chaotic attractor when  $r = 23.5$  with  $(x_0, y_0, z_0, v_0) = (4.9, 4.9, -1.1, 10)$ .

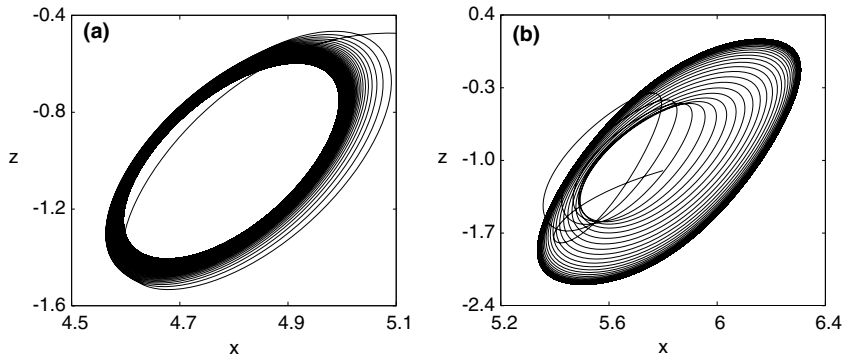


Fig. 3. Stable limit cycles of the controlled Lorenz system (64) around  $C_+$  for  $p=8$ ,  $c=0.5$ ,  $k_c=2.5$  and  $k_n=10$  with  $(x_0, y_0, z_0, v_0) = (5.8, 5.0, -1.1, 10.0)$ , when (a)  $r=24$ ; and (b)  $r=35$ .

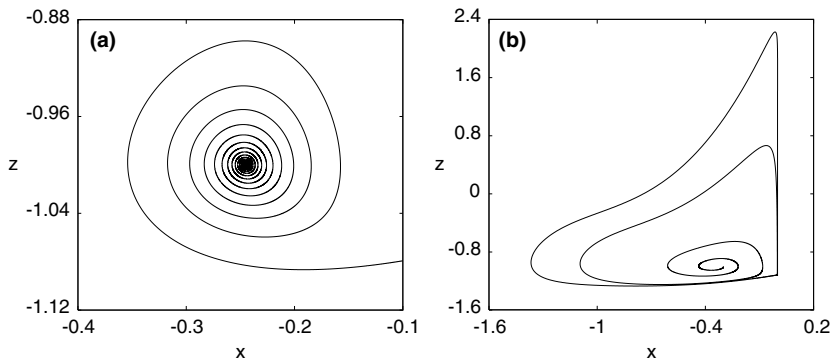


Fig. 4. Trajectories of the controlled Lorenz system (64) around  $C_-$  for  $p=8$ ,  $c=0.5$ ,  $k_c=2.5$  and  $k_n=10$ : (a)  $r=1.06$ , convergent to  $C_-$  with  $(x_0, y_0, z_0, v_0) = (-0.5, -0.5, -1.5, -1.5)$ ; and (b)  $r=1.12$ , convergent to a limit cycle with  $(x_0, y_0, z_0, v_0) = (-0.3, -0.3, -1.1, -0.6)$ .

cycle is stable, as expected, from the analytical prediction. Even for larger values of  $r$ , shown in Fig. 3(b) where  $r=35$ , the numerical result still shows that the periodic solution is stable.

Similarly, Fig. 4 shows the numerical results related to  $C_-$ , when  $p=8$ ,  $c=0.5$ ,  $k_c=2.5$  and  $k_n=10$  (same as that used for Fig. 3), but for smaller  $r$  since  $r_H = 1.06728042$  for  $C_-$ . It is seen that when  $r=1.06 < r_H$ , the trajectory converges to  $C_-$  (see Fig. 4(a)), but to a stable limit cycle when  $r=1.12$ , shown in Fig. 4(b). It has been noted that unlike the periodic solutions bifurcating from  $C_+$ , the limit cycles bifurcating from  $C_-$  are stable only if the values of  $r$  are chosen close to the critical point  $r_H$ . For example, when  $r=1.13$ , the numerical simulation shows that the trajectory diverges to infinity.

#### 4.2. A nonlinear electrical circuit

A nonlinear electrical circuit, shown in Fig. 5, consists of an inductor,  $L$ , two capacitors  $C_1$  and  $C_2$ , two resistors  $R_1$  and  $R_2$ , a tunnel-diode and a conductance. Suppose  $L$ ,  $C_1$ ,  $C_2$ ,  $R_1$  and  $R_2$  are linear components, and in addition,  $R_1$  may be varied. The tunnel-diode and the conductance are nonlinear elements, and they are voltage-controlled. The conductance is a combination of a tunnel-diode and a current-reversing device. The characteristics of the tunnel diode is given by [31] by

$$i_d = f(V_d) \triangleq 0.01776V_d - 0.10379V_d^2 + 0.22962V_d^3 - 0.22631V_d^4 + 0.08372V_d^5. \tag{76}$$

Thus, the characteristics of the conductance is  $i_G = -f(V_G)$ . The current in the inductor and the voltages across the capacitors are chosen as the state variables (as shown in Fig. 5), leading to the following differential equations:

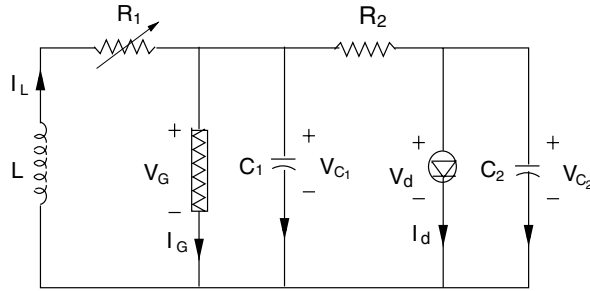


Fig. 5. An electrical circuit.

$$\begin{aligned}
 L \frac{di_L}{dt} &= -R_1 i_L - V_{C_1}, \\
 C_1 \frac{dV_{C_1}}{dt} &= -i_G + i_L - \frac{1}{R_2} (V_{C_1} - V_{C_2}), \\
 C_2 \frac{dV_{C_2}}{dt} &= -i_d + \frac{1}{R_2} (V_{C_1} - V_{C_2}).
 \end{aligned}
 \tag{77}$$

Denoting the state variables  $i_L$ ,  $V_{C_1}$  and  $V_{C_2}$  by  $x$ ,  $y$  and  $z$ , respectively, we may rewrite Eq. (77) as

$$\begin{aligned}
 \frac{dx}{dt} &= -R_1 x - y, \\
 \frac{dy}{dt} &= x - 0.001(y - z) + 0.01776y - 0.10379y^2 + 0.22962y^3 - 0.22631y^4 + 0.08372y^5, \\
 \frac{dz}{dt} &= 0.001(y - z) - 0.01776z + 0.10379z^2 - 0.22962z^3 + 0.22631z^4 - 0.08372z^5,
 \end{aligned}
 \tag{78}$$

where  $L$ ,  $C_1$ ,  $C_2$  and  $R_2$  have been chosen respectively, the values 1, 1, 1 and 1000 in the corresponding units, while  $R_1$  is treated as a control parameter.

System (78) has multiple equilibrium solutions obtained from  $\dot{x} = \dot{y} = \dot{z} = 0$ . In this paper, we only consider bifurcations from the trivial solution  $x = y = z = 0$ , and pay particular attention to Hopf bifurcation. It is easy to obtain the characteristic polynomial of system (78) evaluated at the trivial equilibrium solution as

$$P(\lambda) = \lambda^3 + (0.002 + R_1)\lambda^2 + (0.9996845824 + 0.002R_1)\lambda + 0.01876 - 0.0003154176R_1.$$

Applying the Hurwitz criterion yields the stability condition for the trivial equilibrium:

$$0.0167600020 < R_1 < 59.4767064362.
 \tag{79}$$

Further, it can be shown that a static bifurcation occurs at  $R_1 = 59.4767064362$  while a Hopf bifurcation emerges at  $R_1 = 0.0167600020$ . Suppose the current state of the system is under the selection of  $R_1 = 30$ , and we decrease  $R_1$  until  $R_1 = 0.0167600020$  at which the trivial equilibrium solution becomes unstable and it bifurcates into a family of limit cycles as  $R_1$  further decreases.

**Without control.** First, consider the case without control. To obtain the stability condition using the SNF, let

$$R_1 = 0.0167600020 - \mu,
 \tag{80}$$

and introduce the following transformation  $(x, y, z)^T = Q(\tilde{x}, \tilde{y}, \tilde{z})$ , where  $Q$  is given by

$$Q = \begin{bmatrix} 1.0000431639 & 0.0107620497 & -0.0009999305 \\ -0.0060001928 & -1.0000825710 & -0.0000019999 \\ -0.0009999841 & -0.0000127613 & 1.0000014998 \end{bmatrix},
 \tag{81}$$

under which the transformed system is obtained as

$$\begin{aligned}
 \frac{d\tilde{x}}{dt} &= 0.9998590413\tilde{y} + (1.0000655704\tilde{x} + 0.0107622908\tilde{y} - 0.0009999529\tilde{z})\mu \\
 &\quad - 0.0000000401\tilde{x}^2 - 0.0011171091\tilde{y}^2 + 0.0001037875\tilde{z}^2 - 0.0000134046\tilde{x}\tilde{y} \\
 &\quad - 0.0000002076\tilde{x}\tilde{z} - 0.0000000071\tilde{y}\tilde{z} + \dots,
 \end{aligned}$$



$$\begin{aligned} \frac{d\tilde{y}}{dt} &= -0.9998590413\tilde{x} - (0.0060000928\tilde{x} + 0.0000645705\tilde{y} - 0.0000059994\tilde{z})\mu \\ &\quad + 0.0000037366\tilde{x}^2 + 0.1038052724\tilde{y}^2 - 0.0000008302\tilde{z}^2 + 0.0012456004\tilde{x}\tilde{y} \\ &\quad + 0.0000000042\tilde{x}\tilde{z} + 0.0000004152\tilde{y}\tilde{z} + \dots, \\ \frac{d\tilde{z}}{dt} &= -0.0187600020\tilde{z} + (0.0009999716\tilde{x} + 0.0000107613\tilde{y} - 0.0000009999\tilde{z})\mu \\ &\quad + 0.0000001038\tilde{x}^2 + 0.0000002076\tilde{y}^2 + 0.1037902594\tilde{z}^2 + 0.0000000051\tilde{x}\tilde{y} \\ &\quad - 0.0002075769\tilde{x}\tilde{z} - 0.0000026490\tilde{y}\tilde{z} + \dots, \end{aligned} \tag{82}$$

where  $\dots$  represents higher order terms. The new system clearly shows that its Jacobian evaluated at the origin  $\tilde{x} = \tilde{y} = \tilde{z} = 0$  is in the Jordan canonical form.

Executing the Maple program yields the following SNF:

$$\begin{aligned} \frac{dR}{d\tau} &= R(0.5000005000v + 0.0861699786R^2), \\ \frac{d\Theta}{d\tau} &= 0.9998590408 + 0.0083811918v - 0.3163637547R^2 + \dots \end{aligned} \tag{83}$$

The SNF clearly indicates that a subcritical Hopf bifurcation occurs at the critical point  $v = 0$ , and thus the bifurcating limit cycles are unstable.

**With control.** Now, consider adding a feedback control to system (78). Unlike the first example where a washout filter is introduced, here a direct feedback control is applied. It is required that the control does not change the equilibrium  $x = y = z = 0$ , but convert the subcritical Hopf bifurcation to supercritical. There exist many ways to design the feedback control. We take a simple one, given in the form of

$$u_3 = -k_n y^3, \tag{84}$$

which is added to the third equation of Eq. (78). Then, under the same transformation (80), employing the Maple program to obtain the following SNF for the controlled system:

$$\begin{aligned} \frac{dR}{d\tau} &= R[0.5000005000v + (0.0861699786 - 0.3750754316k_n)R^2], \\ \frac{d\Theta}{d\tau} &= 0.9998590408 + \frac{0.0104785841k_n^2 - 0.0126007750k_n + 0.0726815346}{k_n - 0.2297403970}R^2 + \dots \end{aligned} \tag{85}$$

Thus, as long as

$$\left. \begin{aligned} 0.0861699786 - 0.3750754316k_n < 0 \\ k_n - 0.2297403970 \neq 0 \end{aligned} \right\} \text{ i.e., } k_n > 0.2297403971, \tag{86}$$

the Hopf bifurcation of the controlled system is supercritical.

The numerical simulation results of the electrical circuit are shown in Figs. 6 and 7, respectively for the uncontrolled and controlled systems. It is seen from Figs. 6(a) and 7(a) that the trajectories converge to the origin  $x = y = z = 0$  when

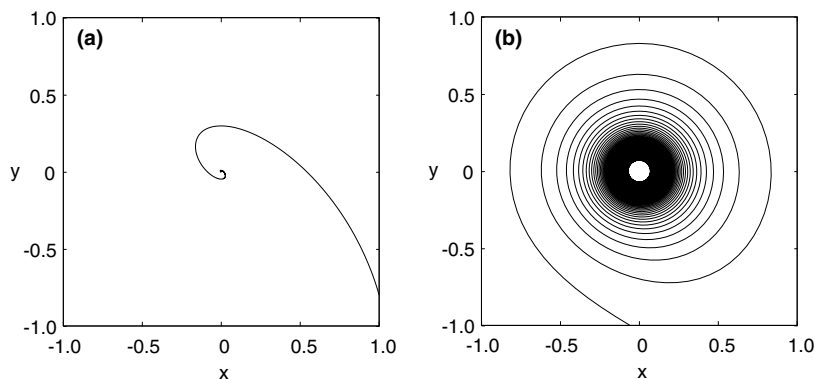


Fig. 6. Trajectories of the uncontrolled electrical circuit: (a)  $R_1 = 1$ , convergent to the origin  $x = y = z = 0$  from the initial point  $(1.0, -0.8, 1.0)$ ; and (b)  $R_1 = 0.012$ , divergent to infinity from the initial point  $(0.05, -0.05, 0.08)$ .

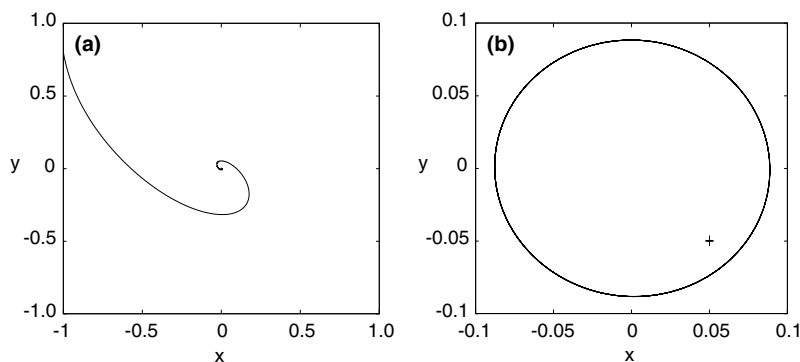


Fig. 7. Trajectories of the controlled electrical circuit for  $k_n = 0.5$ : (a)  $R_1 = 1$ , convergent to the origin  $x = y = z = 0$  from the initial point  $(-1.0, 0.8, -1.0)$ ; and (b)  $R_1 = 0.012$ , convergent to a limit cycle from the initial point  $(0.05, -0.05, 0.08)$ .

$R_1 = 1.0$  (i.e.,  $\mu = -0.983239998$ ) for both controlled and uncontrolled systems. This indicates that the origin  $x = y = z = 0$  is stable when  $\mu < 0$ . However, when  $R_1 = 0.012$  (i.e.,  $\mu = 0.004760002$ ) the trajectory of the uncontrolled system diverges to infinity even from an initial point close to the origin (see Fig. 6(b)) implying that the origin is unstable and the Hopf bifurcation is subcritical; while the trajectory of the controlled system converges to a stable limit cycle (see Fig. 7(b) where only the final limit cycle is shown and the initial point is marked by +). This indeed verifies that the Hopf bifurcation of the controlled system becomes supercritical.

Note that the feedback control (84) changes the second equation of (78) to

$$\frac{dy}{dt} = x - 0.001(y - z) + 0.01776y - 0.10379y^2 - 0.27038y^3 - 0.22631y^4 + 0.08372y^5.$$

It is seen from the above equation that the sign of the third order term has been changed from positive to negative, which renders the subcritical Hopf bifurcation to supercritical.

## 5. Conclusions

An efficient method with symbolic computation has been developed for computing explicit center manifold and the simplest normal form with unfolding for general semi-simple cases, with particular attention given to codimension-one singularities. The method combines center manifold theory and normal form theory into one unified procedure to simultaneously obtain the coefficients of the simplest normal form and nonlinear transformations. It has been shown that in addition to near-identity nonlinear transformation, time rescaling is needed for single zero singularity, while both time and parameter rescaling are required for Hopf bifurcation. The explicit, recursive formulas have been implemented using Maple. The results have been applied to the Lorenz system and a nonlinear electrical circuit to study controlling Hopf bifurcation with a nonlinear state feedback control.

## Acknowledgement

The supports received from the Natural Sciences and Engineering Research Council of Canada (NSERC) and City University of Hong Kong are greatly acknowledged.

## References

- [1] Kang W. Bifurcation and normal form of nonlinear control systems, parts I and II. *SIAM J Contr Optim* 1998;36:193–232.
- [2] Chen G, Moiola JL, Wang HO. Bifurcation control: theories, methods, and applications. *Int J Bifur Chaos* 2000;10:511–48.
- [3] Chen D, Wang HO, Chen G. Anti-control of Hopf bifurcation. *IEEE Trans Circ Sys-I* 2001;48:661–72.
- [4] Chen G, editor. *Controlling chaos and bifurcations in engineering systems*. Boca Raton, FL: CRC Press; 1999.
- [5] Yu P. Bifurcation dynamics in control systems. In: *Bifurcation control: Theory and applications*. Berlin: Springer-Verlag; 2003. p. 99–126.

- [6] Yu P, Chen G. Hopf bifurcation control using nonlinear feedback with polynomial functions. *Int J Bifur Chaos* 2004;14(5):1673–704.
- [7] Chen Z, Yu P. Controlling and anti-controlling Hopf bifurcations in discrete maps using polynomial functions. *Chaos, Solitons & Fractals* 2005;26(4):1231–48.
- [8] Chen Z, Yu P. Hopf bifurcation control for an internet congestion model. *Int J Bifur Chaos* 2005;15(8):2643–51.
- [9] Ushiki S. Normal forms for singularities of vector fields. *Jpn J Appl Math* 1984;1:1–37.
- [10] Baider A, Churchill R. Unique normal forms for planar vector fields. *Math Z* 1988;199:303–10.
- [11] Chua LO, Kokubu H. Normal forms for nonlinear vector fields—Part I: Theory and algorithm. *IEEE Trans Circ Syst* 1988;35:863–80.
- [12] Chua LO, Kokubu H. Normal forms for nonlinear vector fields—Part II: Applications. *IEEE Trans Circ Syst* 1988;36:51–70.
- [13] Sanders JA, van der Meer JC. Unique normal form of the Hamiltonian 1:2-resonance. In: Broer HW, Takens F, editors. *Geometry and analysis in nonlinear dynamics*. Harlow: Longman; 1990. p. 56–69.
- [14] Yu P. Simplest normal forms of hopf and generalized hopf bifurcations. *Int J Bifur Chaos* 1999;9:1917–39.
- [15] Yu P, Yuan Y. The simplest normal form for the singularity of a pure imaginary pair and a zero eigenvalue. *Dynamics of continuous, discrete and impulsive systems, series B: Applications & algorithms* 2000;8b:219–49.
- [16] Wang D, Li J, Huang M, Jiang Y. Unique normal forms of Bogdanov–Takens singularity. *J Differential Equation* 2000;163:223–38.
- [17] Chen G, Dora JD. An algorithm for computing a new normal form for dynamical systems. *J Symb Comput* 2000;29:393–418.
- [18] Yu P, Yuan Y. The simplest normal forms associated with a triple zero eigenvalue of indices one and two. *Nonlinear Anal: Theor Methods Appl* 2001;47(2):1105–16.
- [19] Algaba A, Freire E, Gamero E. Characterizing and computing normal forms using Lie transforms: a survey. *Dynamics of continuous, discrete and impulsive systems series A: Mathematical analysis* 2001;8a:449–75.
- [20] Yuan Y, Yu P. Computation of the simplest normal forms of differential equations associated with a double-zero eigenvalues. *Int J Bifur Chaos* 2001;11(5):1307–30.
- [21] Sanders JA. Normal form theory and spectral sequences. *J Differential Equation* 2003;192:536–52.
- [22] Yu P. Computation of the simplest normal forms with perturbation parameters based on Lie transform and rescaling. *J Comput Appl Math* 2002;144(2):359–73.
- [23] Yu P. A simple and efficient method for computing center manifold and normal forms associated with semi-simple cases. *Dynamics of continuous, discrete and impulsive systems, series B: Applications & algorithms* 2003;10(1–3):273–86.
- [24] Yu P, Yuan Y. An efficient method for computing the simplest normal forms of vector fields. *Int J Bifur Chaos* 2003;13(1):19–46.
- [25] Yu P, Yuan Y. A matching pursuit technique for computing the simplest normal forms of vector fields. *J Symb Comput* 2003;35(5):591–615.
- [26] Yu P, Leung AYT. A perturbation method for computing the simplest normal forms of dynamical systems. *J Sound Vib* 2003;261(1):123–51.
- [27] Carr J. *Applications of center manifold theory*. New York: Springer-Verlag; 1981.
- [28] Yu P. Computation of normal forms via a perturbation technique. *J Sound Vib* 1998;211:19–38.
- [29] Yu P, Leung AYT. The simplest normal form of Hopf bifurcation. *Nonlinearity* 2003;16(1):277–300.
- [30] Guckenheimer J, Holmes P. *Nonlinear oscillations, dynamical systems, and bifurcations of vector fields*. 4th ed. New York: Springer-Verlag; 1993.
- [31] Chua LO. *Introduction to nonlinear network theory*. New York: McGraw-Hill; 1969.